

A Comparison of Three Regions of Puppis A

K.F. Fischbach, L.M. Bateman, C.R. Canizares, T.H. Markert, and P.J. Saez

Massachusetts Institute of Technology, Cambridge, Massachusetts, U.S.A.

ABSTRACT High resolution X-ray spectral observations of Puppis A were performed with the FPCS on the *Einstein* Observatory at three regions of the remnant: the shock front, the bright eastern knot, and the interior. Plasma diagnostics of lines from OVII and OVIII constrain the values of electron temperature, ionization timescale, and hydrogen column density. We compare results of the diagnostics for these three regions. A non-equilibrium analysis of previously published fluxes of oxygen lines shows that the interior has not yet reached ionization equilibrium.

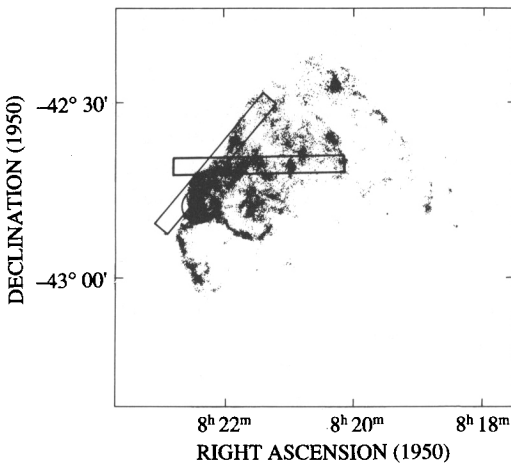


Figure 1 Aperture positions for the bright eastern knot, the shock front and the interior overlaid on an HRI image of Petre, *et al.* (1981).

Between April, 1979 and July, 1980, the Puppis A supernova remnant was observed using the Focal Plane Crystal Spectrometer (FPCS) on the *Einstein* Observatory (Canizares, *et al.* 1979). The remnant was observed at several positions; the bright eastern knot, the shock front, and at several closely spaced positions in the interior. A circular (6 arc minute) aperture was used to observe the bright eastern knot; in the other cases a 3 X 30 arc minute rectangular aperture was used to make the observations. The interior was observed with the rectangular aperture in a variety of angular orientations. Figure 1 shows FPCS aperture positions for the three regions, overlaid on the Puppis A image obtained by Petre *et al.* (1981). The X-ray observations consisted primarily of lines of helium-like and hydrogen-like ions of oxygen (O VII and O VIII) and neon (Ne IX and Ne X), and neon-like iron (Fe XVII).

The X-ray emission lines detected by the FPCS provide useful diagnostics of conditions in the line-emitting plasma. For transitions $i \rightarrow g$ and $j \rightarrow k$ of ionization states $+x$ and $+y$ of an element Z, the ratio of X-ray fluxes is given by:

$$\frac{f_{ig}}{f_{jk}} = \frac{\Omega_{ig} \times n_{+x} \times \exp(-\sigma(E_{ig})N_H) \times \exp(-E_{ig}/(kT_e))}{\Omega_{jk} \times n_{+y} \times \exp(-\sigma(E_{jk})N_H) \times \exp(-E_{jk}/(kT_e))}$$

where Ω_{ig} is the effective collision strength for transition $i \rightarrow g$, E_{ig} is the excitation energy, T_e the electron temperature, n_{+x} the density of ion x , σ the cross-section per hydrogen atom for photoelectric absorption at energy E_{ig} , and N_H the hydrogen column

density (see Vedder *et al.* 1986). Since it is difficult to make enough measurements so as to solve for all of the unknowns, the approach we have taken is to measure a few line intensities selected so that as many parameters as possible will cancel. For example, two lines from the same ion define an allowed region in the parameter space of column density N_H and electron temperature T_e . In order to use two different ions from the same atom, it is necessary to perform a non-equilibrium analysis because the relative abundances of the various ions are functions of time since the plasma was shocked. The ionization structure is determined by solving a set of $Z+1$ simultaneous differential equations. (We have employed the technique of Hughes and Helfand (1985) to solve the ion balance equations.) The resulting ion abundances are then used explicitly in the equations for the line emissivities. The various parameters of the non-equilibrium model are T_e , N_H , and τ . Here τ (\equiv electron density \times time since the shock) is the ionization timescale and measures the extent to which ionization equilibrium has been attained. The complete analysis technique is discussed in more detail in Markert *et al.* (1988).

In order to compare the physical conditions of the three regions, (i.e. interior, bright eastern knot and shock front) we compared the results of the analysis described above (Winkler *et al.* 1981; Winkler *et al.* 1983; Fischbach *et al.* 1988). The derived allowable regions in (N_H, T_e) and (T_e, τ) parameter space are reproduced in Figures 2, 3 and 4 for the respective regions. In order to obtain an estimate of the ionization timescale, τ , of the interior, previously published oxygen line fluxes (Winkler *et al.* 1981) were applied to the non-equilibrium analysis, from which Figure 2b is obtained. In the analysis N_H was assumed to be $4 \times 10^{21} \text{ cm}^{-2}$, but the results are not particularly sensitive to this assumption.

The deduced constraints on column density N_H , electron temperature T_e , and ionization timescale τ are shown in Table 1 for the three regions.

TABLE 1
PLASMA DIAGNOSTICS

Region	T (10^6 K)	τ (yr cm^{-3})	t (yr) ⁽¹⁾	n_e (cm^{-3}) ⁽²⁾
Interior	4.3-19 ⁽³⁾	300-2000	3700	0.1-0.6
Eastern Knot	6-8	800-1200	100	8-12
Shock Front	>7.9	150-400	100	1.5-4

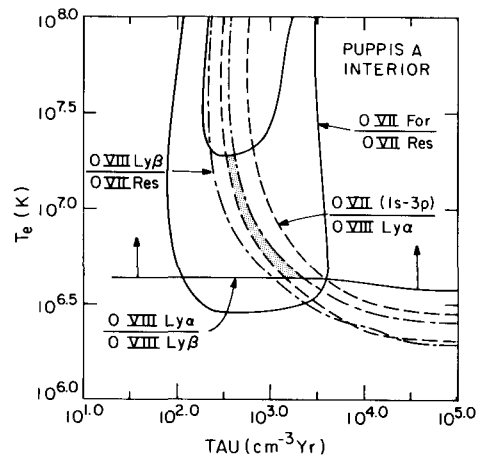
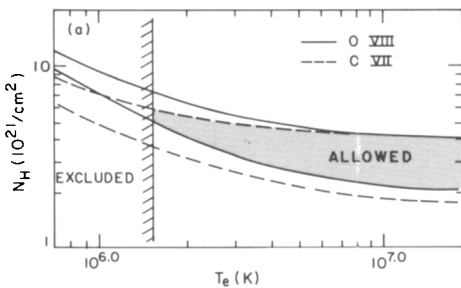
- (1) See Winkler *et al.*, 1988; Winkler *et al.*, 1983; Fischbach *et al.*, 1988).
- (2) Electron density n_e is estimated by naively assuming $\tau = n_e t$. In fact, the line-emitting region consists of material shocked at different times, so the reported value of n_e is probably a slight underestimate.
- (3) Winkler (1981) derives $T_e \geq 1.5 \times 10^6$. These temperature constraints are obtained from the analysis shown in Figure 2b.

The non-equilibrium analysis on oxygen lines from the interior suggests that the plasma departs substantially from ionization equilibrium. Thus, none of the three regions is found to be in ionization equilibrium despite the advanced age (~ 3700 years) of the remnant.

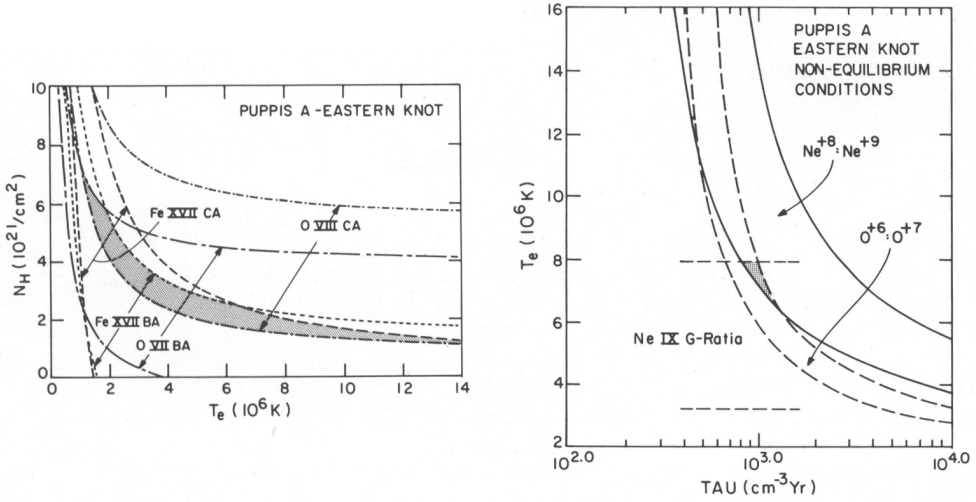
Acknowledgements We thank Jack Hughes for supplying his computer code for the non-equilibrium analysis. We are grateful to Elaine Aufiero for preparing the manuscript. This work was supported in part by NASA grant NAG 8-494.

REFERENCES

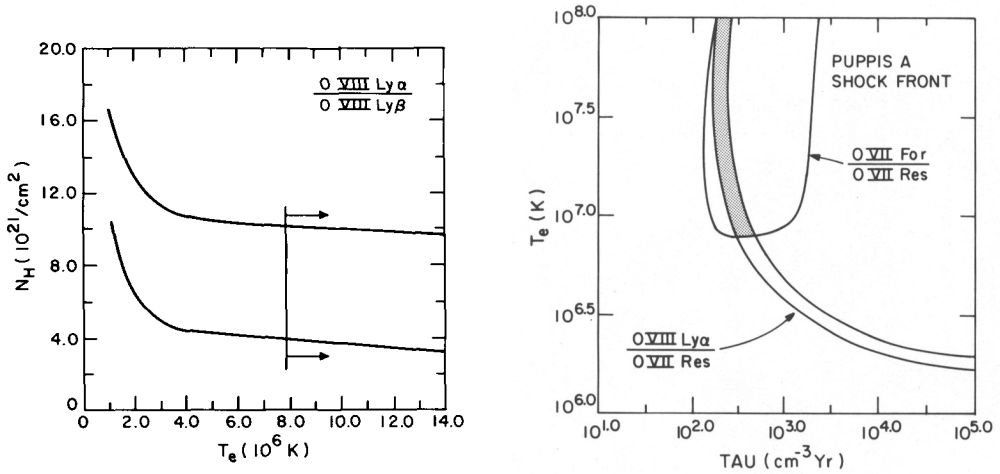
- Canizares, C.R., Clark, G.W., Markert, T.H., Berg, C., Smedira, M., Bardas, D., Schnopper, H., and Kalata, K. 1979, *Ap. J. (Letters)*, **234**, L33.
 Fischbach, K.F., Canizares, C.R., Markert, T.H., and Coyne, J.M. 1988, in *Supernova Remnants and the Interstellar Medium*, eds. R.S. Roger and T.L. Landecker, (Cambridge University Press, Cambridge) 153.
 Hughes, J.P. and Helfand, D.J. 1985, *Ap. J.*, **291**, 544.
 Markert, T.H., Blizzard, P.L., Canizares, C.R. and Hughes, J.P. 1988, in *Supernova Remnants and the Interstellar Medium*, eds. R.S. Roger and T.L. Landecker, (Cambridge University Press, Cambridge) 129.
 Petre, R., Canizares, C.R., Kriss, G.A. and Winkler, P.F. 1981, *Ap. J.*, **258**, 22.
 Vedder, P.W., Canizares, C.R., Markert, T.H. and Pradhan, A.K. 1986, *Ap. J.*, **307**, 269.
 Winkler, P.F., Canizares, C.R., Clark, G.W., Markert, T.H., Petre, R. 1981, *Ap. J.*, **245**, 574.
 Winkler, P.F., Canizares, C.R. and Bromley, B.C. 1983, in *Supernova Remnants and Their X-Ray Emission*, eds. J. Danziger and P. Gorenstein, (Dordrecht: Reidel), 245.
 Winkler, P.F., Tuttle, J.H., Kirshner, R.P. and Irwin, M.J. 1988, in *Supernova Remnants and the Interstellar Medium*, eds. R.S. Roger and T.L. Landecker, (Cambridge University Press, Cambridge 65.)



Figures 2a,b Regions in (N_H, T_e) and (T_e, τ) parameter space allowed by FPCS measurements of the interior. Shaded area is region of overlap consistent with all measurements. Figure 2a is reproduced from Winkler *et al.* (1981). Figure 2b shows results of a non-equilibrium analysis using oxygen lines as published in Winkler *et al.* (1981) and assuming $N_H = 4 \times 10^{21} \text{ cm}^{-2}$. Each pair of contours in Figure 2b indicates 90% confidence.



Figures 3a,b Allowed (shaded) regions in (N_H, T_e) and (T_e, τ) parameter space for the bright eastern knot (Winkler et al. 1983).



Figures 4a,b Allowed (shaded) regions in (N_H, T_e) and (T_e, τ) parameter space for the shock front (Fischbach et al. 1988). Arrows to the right of the vertical line in Figure 3a indicate allowed region.